

## Comparison of large-scale amplitude modulation in turbulent boundary layers, pipes, and channel flows

Romain Mathis, Jason P. Monty, Nicholas Hutchins, and Ivan Marusic

Department of Mechanical Engineering, University of Melbourne, Victoria 3010, Australia

(Received 16 August 2009; accepted 26 October 2009; published online 24 November 2009)

Recent investigations by Monty *et al.* [J. Fluid Mech. **632**, 431 (2009)] showed that important modal differences exist between channels/pipes and boundary layers, mainly in the largest energetic scales. In addition, Mathis *et al.* [J. Fluid Mech. **628**, 311 (2009)] recently reported and quantified a nonlinear scale interaction in zero-pressure gradient turbulent boundary layers, whereby the large-scale motion amplitude modulates the small-scale motions. In this study, a comparison of this modulation effect of the streamwise velocity component is undertaken for all three flows for matched Reynolds number and measurement conditions. Despite the different large-scale phenomena in these internal and external wall-bounded flows, the results show that their amplitude modulation influence remains invariant in the inner region with some differences appearing in the outer region. © 2009 American Institute of Physics. [doi:10.1063/1.3267726]

The behavior of canonical wall-bounded shear flow in pipes, channels, and boundary layers has been well documented over the past few decades.<sup>1–5</sup> A recent investigation by Monty *et al.*,<sup>6</sup> comparing turbulent boundary layers (TBLs) with channel and pipe flows at matched Reynolds number, has given new insight into internal (channel/pipe) and external (boundary layer) flow structures. By analyzing energy spectra maps of streamwise velocity fluctuation for all three flows, Monty *et al.*<sup>6</sup> showed that a very good agreement exists between channel and pipe flows, whereas significant differences between channels/pipes and boundary layers have been highlighted. These differences were found to reside in the largest scales, which present a bimodal characteristic in the outer part of channel/pipe flows, contrary to boundary layers where only one mode exists. Kim and Adrian<sup>7</sup> and Guala *et al.*<sup>8</sup> discussed previously the possible mechanisms responsible for these significant changes between internal and external flows. Furthermore, Mathis *et al.*<sup>9</sup> showed for boundary layers that the large-scale events are not merely superimposed onto the small-scale motions, but also amplitude modulate them. Moreover, they have observed an increase in the amplitude modulation (AM) as the Reynolds number increases. Based on the observation that the large-scale motions (LSMs) are structurally different between channels/pipes and boundary layer flows, it is then logical to consider what this means in terms of the modulation of the small-scale events by the LSMs.

We report the results from three different facilities located at the University of Melbourne in which the Kármán number  $Re_\tau$  was matched. The Kármán number (or friction Reynolds number) is defined as the ratio of the outer to the viscous length scales,  $Re_\tau = \delta U_\tau / \nu$ . The boundary layer tunnel has a working test section of dimensions  $27 \times 2 \times 1$  m<sup>3</sup>, with a low free-stream turbulence intensity, nominally 0.05%. A fully description of the facility is available in Nickels *et al.*<sup>10</sup> The fully developed channel and pipe flow facilities are detailed in Monty *et al.*<sup>11</sup> The channel has an aspect

ratio of 11.7:1, minimizing the side-wall influence. Further details of the experimental conditions are given in Table I and in Monty *et al.*<sup>6</sup> The outer length-scale  $\delta$  corresponds either to the boundary layer thickness (calculated from a modified Coles law of the wake fit<sup>12</sup>), the half-height of the channel, or the radius of the pipe.  $U_\tau$  is the friction velocity and  $\nu$  is the kinematic viscosity. Measurements were made by traversing single-normal hot-wire probes (Wollaston wire with Dantec 55P05 probe in the TBL and Dantec 55P15 probe in the channel/pipe). In all cases, the probe was operated in constant temperature mode with overheat ratio set to 1.8. To avoid spatial resolution issues when comparing the different flows, a nondimensional hot-wire length of  $l^+ = 30$  was maintained for all three flows ( $l^+ = l U_\tau / \nu$ , where  $l$  is the length of the etched part of the hot wire). It should be noted that  $U_\tau$  is accurately calculated from pressure drop in the channel and pipe flows, whereas the Clauser chart is used in the boundary layer (with log law constants  $\kappa = 0.41$  and  $A = 5.0$ ).

Figure 1 displays the premultiplied streamwise energy spectra map plotted against the wall distance and wavelength for all three flows, as shown by Monty *et al.*<sup>6</sup> Contour levels are formed from two dimensional premultiplied energy spectra  $k_x \phi_{uu} / U_\tau^2$  obtained at each wall normal location  $z^+$ . The qualitative overview of the spectra looks similar. An energetic peak occurs in the near-wall region (called the “inner peak”), which is the signature of the viscous-scaled near-wall cycle of elongated high- and low-speed streaks.<sup>13</sup> As we move away from the wall, a secondary peak appears in the logarithmic region (referred to as the “outer peak”)<sup>14</sup> corresponding to the superstructure-type events associated with the log region.<sup>15</sup> Hutchins and Marusic<sup>15,16</sup> showed that this large-scale structure imposes a strong “footprint” at the wall with low-wavenumber events superimposed on the high frequency streamwise fluctuations of the near-wall cycle. Mathis *et al.*<sup>9</sup> conclusively showed that this footprint amplitude modulates the small scales. Well into the outer flow

TABLE I. Experimental parameters for TBL, channel, and pipe.

Facility	Flow conditions					Hot-wire details			Acquisition details			
	$Re_\tau$	$x$ (m)	$U_\infty$ ( $ms^{-1}$ )	$\delta$ (m)	$\nu/U_\tau$ ( $\mu m$ )	$l$ (mm)	$d$ ( $\mu m$ )	$l^+$	$\Delta t^+$	$f$ (kHz)	$TU_\infty/\delta$ ( $10^4$ )	Symbol
TBL	3020	5.0	12.5	0.1003	33.2	1	5.0	30	0.57	24	2.25	$\triangle$
Channel	3015	17.6	23.1	0.05	16.7	0.5	2.5	30	0.55	100	2.77	$\square$
Pipe	3005	17.3	24.3	0.0494	16.4	0.5	2.5	30	0.56	100	2.95	$\circ$

( $z/\delta > 0.3$ ) the energy signature of the large scales moves to smaller wavelength ( $\lambda_x/\delta \approx 3$ ) in the boundary layer, whereas two peaks can be distinguished in channel and pipe maps [respectively highlighted in Fig. 1 by bold lines labeled

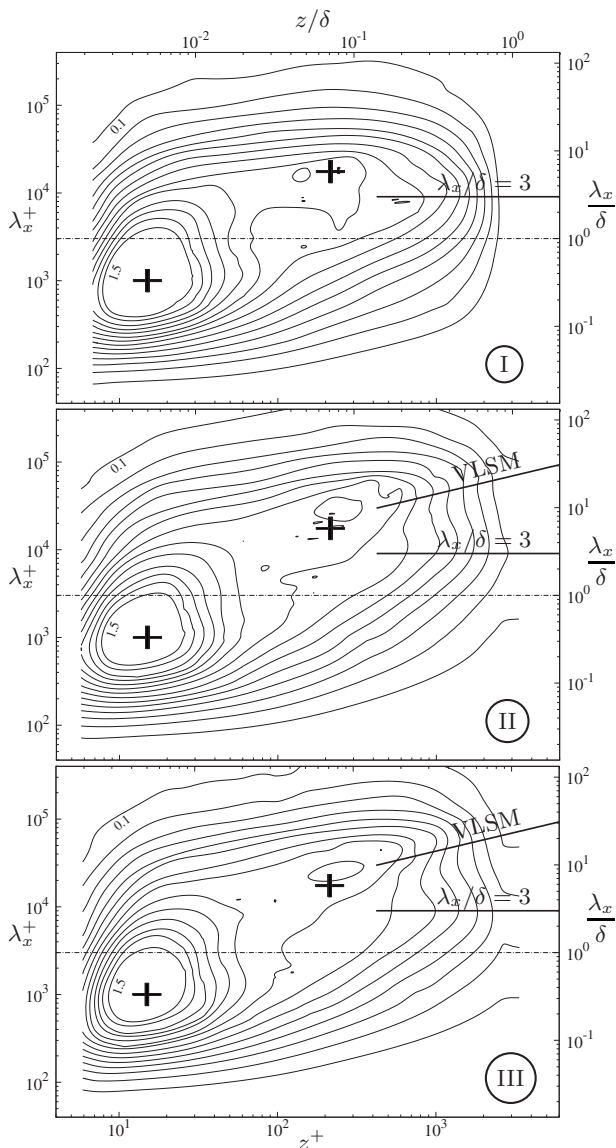


FIG. 1. Isocontour representation of the premultiplied energy spectra of streamwise velocity fluctuations  $k_x \phi_{uu}/U_\tau^2$  for (i) TBL, (ii) channel, and (iii) pipe at matched  $Re_\tau$ . Levels are from 0.1 to 1.5 in steps of 0.1 (levels 0.1 and 1.5 are labeled). The + symbol marks the inner ( $z^+ \approx 15$ ,  $\lambda_x^+ \approx 1000$ ) and outer peaks ( $z/\delta \approx 3.9$   $Re_\tau^{-1/2}$ ,  $\lambda_x/\delta \approx 6$ ) as identified by Ref. 9. The horizontal dot-dashed line shows the location of the spectral filter ( $\lambda_x = \delta$ ). Adapted from Ref. 6.

$\lambda_x/\delta = 3$  and VLSM (VLSM denotes very-large-scale motion)]. The shorter mode in channel/pipe corresponds to the boundary layer mode at  $\lambda_x/\delta \approx 3$  (identified as LSM in internal flows by Adrian *et al.*<sup>17</sup>). The second peak occurs at much longer wavelengths,  $14 < \lambda_x/\delta < 20$ , identified by Kim and Adrian<sup>7</sup> as the VLSMs. It should be noted, as clearly pointed out in Ref. 6, that superstructures in a boundary layer and VLSM in channel/pipe flows should not be confused. Even if they present similar structural characteristics, VLSM occurs at more distant wall-normal locations and longer wavelengths than superstructures. Furthermore, by studying differences in the energy map between channels/pipes and boundary layers, Monty *et al.*<sup>6</sup> showed that differences reside not only in the outer/core region but extend right down to the wall. This is expected since it is now known that the largest modes from the outer/core region impose their footprint in the near-wall region.<sup>15</sup> However, the fact that the turbulence intensity remains identical in most of the flow ( $\lambda_x/\delta < 0.5$ ) while different energetic distributions are observed suggests that all three flows might have similar qualitative structure with different energetic distributions between shorter and longer scales. Hence, the question arises: Is the AM imparted by the big structures onto the small events, shown by Ref. 9 in boundary layers, similar or different in the channel/pipe flows?

A first approach to study the scale relationship is to decompose a fluctuating velocity signal into a large- and a small-scale component by applying a wavelength pass filter below and above a carefully chosen cutoff wavelength.<sup>16</sup> Spectral energy maps are useful to choose the adequate cutoff wavelength (Fig. 1);  $\lambda_x = \delta$  appears to be a reasonable location to separate large- and small-scale components (filter parameters are given in Table II). An example of the resulting decomposition is given in Fig. 2 for all three flows at wall-normal location  $z^+ = 15$ . The raw signal  $u^+$  is decomposed into a large- $u_L^+$  ( $\lambda_x > \delta$ ) and small-scale  $u_S^+$  ( $\lambda_x < \delta$ ) component [Figs. 2(a) and 2(b)]. The overall observation in Fig. 2 is that whatever the flow, internal or external, an AM effect from the large scales onto the small-scale component is visible. This is highlighted by the sections of signal marked with dashed lines where lower fluctuations of the small-scale component are observed under a large negative excursion of the large-scale component. It should be noted that the present decomposition does not differentiate LSM and VLSM in internal flows.

By using the Hilbert transformation applied to the small-scale component  $u_S^+$ , it is possible to characterize this AM effect.<sup>9</sup> The Hilbert transformation<sup>18,19</sup> is well known to ex-

TABLE II. Definition of filter parameters for scale decomposition.

Subscript	Designation	Spatial filter cutoff
L	Large scales	$\lambda_x/\delta > 1$
S	Small scales	$\lambda_x/\delta < 1$

tract the envelope of any signal, which in AM processing corresponds to the modulating signal<sup>20</sup> (assumed here to be the large-scale component). Hence, a direct evaluation of the modulation is obtained by calculating the correlation coefficient between the envelope of the small-scale component and the large-scale component. However, the envelope returned by the Hilbert transformation will track not only the large-scale modulation due to the log-region events, but also the small-scale variation in the signal.<sup>9</sup> This effect is removed by filtering the envelope at the same cutoff wavelength as the large-scale signal ( $\lambda_x > \delta$ ). The filtered envelope  $E_L(u_S^+)$ , describing the modulation, can now be correlated with the large-scale velocity fluctuation  $u_L^+$ ,

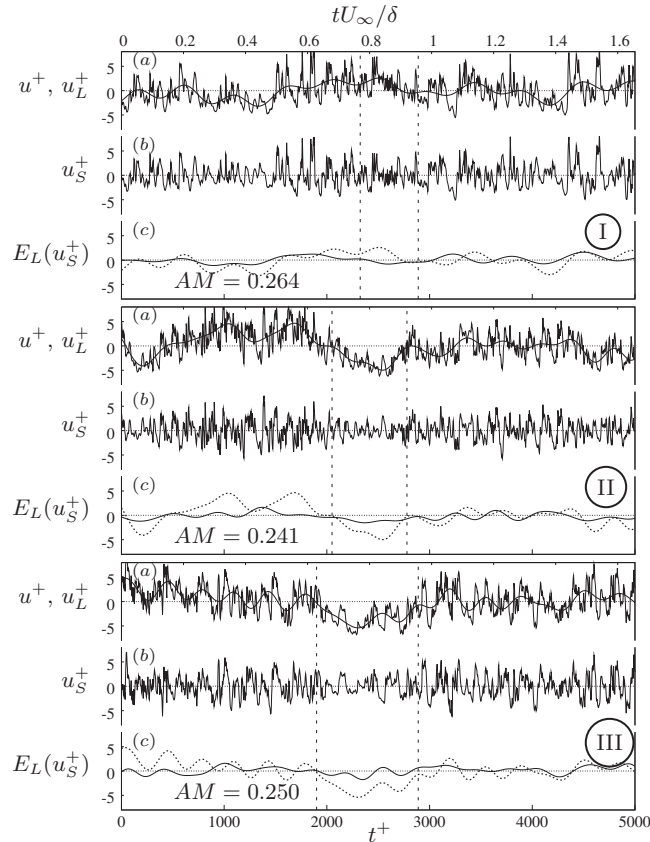


FIG. 2. Example of small-scale decomposition on fluctuating  $u^+$  velocity signal in the near-wall region ( $z^+ \approx 15$ ) for (i) TBL, (ii) channel, and (iii) pipe flows: (a) raw fluctuating component  $u^+$  and large-scale fluctuation  $\lambda_x/\delta > 1$ ; (b) small-scale fluctuation  $\lambda_x/\delta < 1$ ; and (c) filtered envelope (solid line) against the large-scale component (dashed line). For comparison, the mean of the filtered envelope has been adjusted to zero. Dashed vertical lines show regions of negative large-scale fluctuations.

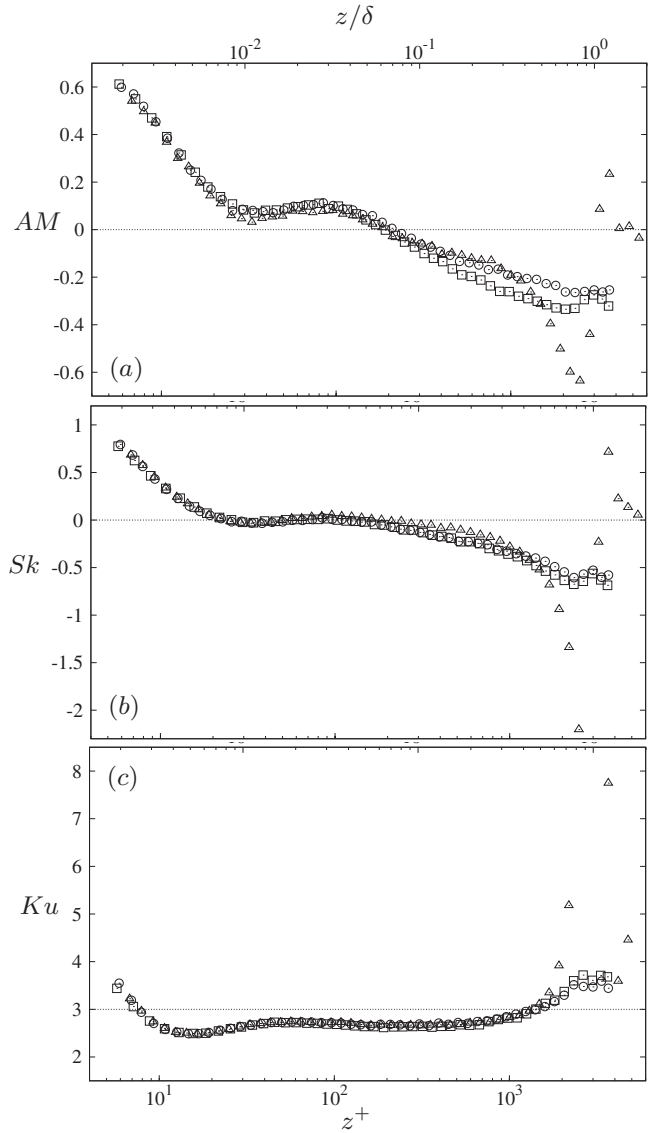


FIG. 3. (a) Wall-normal distribution of the degree of AM, (b) skewness, and (c) kurtosis profiles for ( $\Delta$ ) TBL, ( $\square$ ) channel, and ( $\circ$ ) pipe.

$$AM = \frac{\overline{u_L^+ E_L(u_S^+)}}{\sqrt{\overline{u_L^{+2}} \sqrt{\overline{E_L(u_S^+)^2}}}}, \quad (1)$$

where  $\sqrt{\overline{u^2}}$  denotes the rms value of the signal  $u$ . A complete description of the procedure to characterize the degree of AM of the large scales onto the small scales is available in Ref. 9. For the samples shown in Fig. 2(c), a significant degree of AM is found,  $AM \approx 0.24$ – $0.26$ , for all three flows.

A complete evaluation of the degree of AM across the TBL, channel, and pipe is obtained by applying the procedure for the streamwise fluctuating velocity component  $u^+$  at all wall-normal locations  $z^+$ . The resulting  $AM(z^+)$  for the three flows is presented in Fig. 3(a). A good agreement of AM is observed up to the edge of the logarithmic region ( $z/\delta < 0.15$ ). The fact that the LSMs, either superstructure or VLSM, induce the same AM effect onto the near-wall region agrees with the conclusion of Monty *et al.*<sup>6</sup> that all three flows are of the same type of structure, with only different energetic distribution between small and large scales (pro-

ducing the difference observed in the premultiplied energy spectra maps). Hence, in terms of flow control (for drag reduction purposes), the same strategy acting on the large-scale events would probably give similar benefit for the three flows. Well into the outer/core region ( $z/\delta > 0.3$ ),  $AM(z^+)$  shows a different behavior for all three flows. This is expected as the flows have quite different outer regions due to the opposite wall in internal flow or the intermittency of the wake region in boundary layer. However, even channel and pipe depict different degrees of AM, despite the fact that statistics and energy maps present a very good agreement, including the skewness and flatness profiles [Figs. 3(b) and 3(c)]. In any case, the geometry of channels and pipes is very different, so it is perhaps not surprising that AM is also different. Furthermore, a closer analysis of the spectral profiles by Monty *et al.*<sup>6</sup> at  $z^+ = 2000$  shows that the large scales are weaker in pipes than in channels. This is consistent with the present observations that AM is higher in channels,  $AM(z^+ = 2000) \approx -0.34$ , than in a pipe,  $AM(z^+ = 2000) \approx -0.26$ . In the boundary layer, AM has a very different behavior than in channels/pipes in the outer region ( $z/\delta > 0.5$ ). In Fig. 3(a) a high negative peak ( $AM \approx -0.6$ ) is observed at about  $z^+ \approx 2500$ , which is caused by the intermittency region. Indeed, above  $z/\delta > 0.5$  all small-scale fluctuations appear only within a large negative excursion marking the passage of superstructure-type events. This corresponds to the strong anticorrelation observed at  $z^+ \approx 2500$  consistent with high negative skewness and high positive kurtosis observed at the same location [as seen in Figs. 3(b) and 3(c)], and these are well known characteristics of the intermittency region. Finally, further differences between boundary layers and channel/pipe flows may be revealed by studying the other velocity fluctuating components. Indeed, Hutchins and Marusic<sup>16</sup> showed that not only the streamwise velocity fluctuations seem to be modulated, but all components, as well as the Reynolds shear-stress fluctuations.

We gratefully acknowledge the financial support of the Australian Research Council through Grant Nos. DP0663499, FF0668703, and DP0984577.

- <sup>1</sup>J. C. Rotta, "Turbulent boundary layers in incompressible flow," *Prog. Aerosp. Sci.* **2**, 1 (1962).
- <sup>2</sup>H. Tennekes and J. L. Lumley, *A First Course in Turbulence* (MIT, Cambridge, MA, 1972).
- <sup>3</sup>M. Wosnik, L. Castillo, and W. K. George, "A theory for turbulent pipe and channel flows," *J. Fluid Mech.* **421**, 115 (2000).
- <sup>4</sup>Y. Wu and K. T. Christensen, "Population trends of spanwise vortices in wall turbulence," *J. Fluid Mech.* **568**, 55 (2006).
- <sup>5</sup>W. K. George and L. Castillo, "Zero-pressure-gradient turbulent boundary layer," *Appl. Mech. Rev.* **50**, 689 (1997).
- <sup>6</sup>J. P. Monty, N. Hutchins, H. C. H. Ng, I. Marusic, and M. S. Chong, "A comparison of turbulent pipe, channel and boundary layer flows," *J. Fluid Mech.* **632**, 431 (2009).
- <sup>7</sup>K. C. Kim and R. J. Adrian, "Very large-scale motion in the outer layer," *Phys. Fluids* **11**, 417 (1999).
- <sup>8</sup>M. Guala, S. E. Hommema, and R. J. Adrian, "Large-scale and very-large-scale motions in turbulent pipe flow," *J. Fluid Mech.* **554**, 521 (2006).
- <sup>9</sup>R. Mathis, N. Hutchins, and I. Marusic, "Large-scale amplitude modulation of the small-scale structures in turbulent boundary layers," *J. Fluid Mech.* **628**, 311 (2009).
- <sup>10</sup>T. B. Nickels, I. Marusic, S. Hafez, and M. S. Chong, "Evidence of the  $k^{-1}$  law in high-Reynolds number turbulent boundary layer," *Phys. Rev. Lett.* **95**, 074501 (2005).
- <sup>11</sup>J. P. Monty, J. A. Stewart, R. C. Williams, and M. S. Chong, "Large-scale features in turbulent pipe and channel flows," *J. Fluid Mech.* **589**, 147 (2007).
- <sup>12</sup>M. B. Jones, I. Marusic, and A. E. Perry, "Evolution and structure of sink-flow turbulent boundary layers," *J. Fluid Mech.* **428**, 1 (2001).
- <sup>13</sup>S. J. Kline, W. C. Reynolds, F. A. Schraub, and P. W. Rundstadler, "The structure of turbulent boundary layers," *J. Fluid Mech.* **30**, 741 (1967).
- <sup>14</sup>It should be noted that the outer peak in Fig. 1 is marked as defined by Hutchins and Marusic (Ref. 15) and Mathis *et al.* (Ref. 9) ( $z^+ \approx 3.9 \text{ Re}_\tau^{1/2}$ ,  $\lambda_x/\delta \approx 6$ ), and does not perfectly coincide with the contour lines, likely due to the broad nature of the peak.
- <sup>15</sup>N. Hutchins and I. Marusic, "Evidence of very long meandering features in the logarithmic region of turbulent boundary layers," *J. Fluid Mech.* **579**, 1 (2007).
- <sup>16</sup>N. Hutchins and I. Marusic, "Large-scale influences in near-wall turbulence," *Philos. Trans. R. Soc. London, Ser. A* **365**, 647 (2007).
- <sup>17</sup>R. J. Adrian, C. D. Meinhart, and C. D. Tomkins, "Vortex organization in the outer region of the turbulent boundary layer," *J. Fluid Mech.* **422**, 1 (2000).
- <sup>18</sup>J. S. Bendat and A. G. Piersol, *Random Data: Analysis and Measurement Procedure*, 2nd ed. (Wiley Interscience, New York, 1986).
- <sup>19</sup>A. Papoulis, *The Fourier Integral and Its Applications* (McGraw-Hill, New York, 1962).
- <sup>20</sup>R. Mathis, N. Hutchins, and I. Marusic, "Evidence of large-scale amplitude modulation on the near-wall turbulence," *16th Australasian Fluid Mechanics Conference*, Gold Coast, Australia, edited by P. Jacobs, P. McIntyre, M. Cleary, D. Buttsworth, D. Mee, R. Clements, R. Morgan, and C. Lemckert (School of Engineering, The University of Queensland, Brisbane, 2007).